Title

Genome mining and biosynthesis of a polyketide from a biofertilizer fungus that can facilitate reductive iron assimilation in plant

Journal

Proceedings of the National Academy of Sciences of the United States of America, 116(12)

ISSN

0027-8424

Authors

Chen, Mengbin
Liu, Qikun
Gao, Shu-Shan
et al.

Publication Date

2019-03-19

DOI

10.1073/pnas.1819998116

Peer reviewed

Genome mining and biosynthesis of a polyketide from a biofertilizer fungus that can facilitate reductive iron assimilation in plant

Mengbin Chen[a], Qikun Liu[b,c], Shu-Shan Gao[a], Abbegayle E. Young[a], Steven E. Jacobsen[b,c], and Yi Tang[a,d,1]

[a]Department of Chemical and Biomolecular Engineering, University of California, Los Angeles, CA 90095; [b]Department of Molecular Cell and Developmental Biology, University of California, Los Angeles, CA 90095; [c]Howard Hughes Medical Institute, University of California, Los Angeles, CA 90095; and [d]Department of Chemistry and Biochemistry, University of California, Los Angeles, CA 90095

Edited by Chaitan Khosla, Stanford University, Stanford, CA, and accepted by Editorial Board Member Stephen J. Benkovic February 11, 2019 (received for review November 22, 2018)

Fungi have the potential to produce a large repertoire of bioactive molecules, many of which can affect the growth and development of plants. Genomic survey of sequenced biofertilizer fungi showed many secondary metabolite gene clusters are anchored by iterative polyketide synthases (IPKSs), which are multidomain enzymes noted for generating diverse small molecules. Focusing on the biofertilizer *Trichoderma harzianum* t-22, we identified and characterized a cryptic IPKS-containing cluster that synthesizes tricholignan A, a redox-active *ortho*-hydroquinone. Tricholignan A is shown to reduce Fe(III) and may play a role in promoting plant growth under iron-deficient conditions. The construction of tricholignan by a pair of collaborating IPKSs was investigated using heterologous reconstitution and biochemical studies. A regioselective methylation step is shown to be a key step in formation of the *ortho*-hydroquinone. The responsible methyltransferase (MT) is fused with an N-terminal pseudo-acyl carrier protein (ψACP), in which the *apo* state of the ACP is essential for methylation of the growing polyketide chain. The ψACP is proposed to bind to the IPKS and enable the *trans* MT to access the growing polyketide. Our studies show that a genome-driven approach to discovering bioactive natural products from biofertilizer fungi can lead to unique compounds and biosynthetic knowledge.

iterative polyketide synthase | biosynthesis | natural products | biofertilizer

Human beings have exploited beneficial plant–fungi relationships in agroecosystems since antiquity (1). Field studies, together with model plant studies, have shown that the presence of beneficial fungi can promote plant growth in challenging environments (2, 3). Fungi secrete lytic enzymes, hydrophobins, and metabolites that help plants scavenge nutrients and fight off pathogens (1). Fungal natural products are particularly important in plant–fungi interactions because of their rich biological properties (4, 5). Currently, the most practiced method to exploit beneficial natural products is to apply the producing microorganisms directly on plants or as soil amendments. A major limitation of this approach is that biosynthesis of natural products by fungi can be significantly affected by environmental variations, ranging from soil salinity to plant types. As a result, not all beneficial natural products can be produced under field conditions, while unintended production of mycotoxins may cause harm to the plants (6). A more direct approach is to identify potential metabolites that can be synthesized by fungi under axenic laboratory conditions and elucidate their mode of action, followed by application of the natural product or derivatives to the plant. Through genome sequencing and bioinformatic analysis, it is accepted that most fungi only produce a small fraction (<10%) of natural products under laboratory conditions compared with the number of biosynthetic gene clusters encoded (7). Recent advances in fungal genome mining tools have led to the specific and global activation of biosynthetic gene clusters as a step toward realizing the biosynthetic potential (8, 9). These approaches therefore hold significant promise in identifying new fungal natural products that are beneficial to plant growth, and may lead to applications in agriculture.

Trichoderma harzianum t-22 is a biofertilizer fungus that is widely applied to plants from gardening to agriculture (1). *T. harzianum* t-22 can be found as a dissociative rhizosphere resident or plant endophyte that penetrates the outer layers of the epidermis without causing any invasive harm (10). *T. harzianum* t-22 synthesizes and secretes small molecules that are beneficial to plants, including polyketides that are pathogen antagonists and plant growth regulators (11). Genome sequencing of *T. harzianum* t-22 showed the strain encodes 25 clusters that are anchored by iterative polyketide synthases (IPKSs), far exceeding the number of known polyketides produced by this fungus. Therefore, we reasoned a genome-based approach to mine the IPKS-containing gene clusters in *T. harzianum* t-22 may reveal new natural products that play roles in plant–fungi interactions.

IPKSs are multidomain enzymes that function iteratively to synthesize the core structures of polyketides using primarily malonyl-CoA as the building block (12). While the domain arrangement of IPKSs resembles closely that of fatty acid synthases (FASs), more complex biochemical programming rules lead to diverse structures and complicate structural prediction (13). For example, the tailoring domains, including ketoreductase, dehydratase, enoylreductase, and methyltransferase (MT), function with finely tuned permutations in each iteration to diversify the

Significance

Extensively used as a biofertilizer in agriculture, *Trichoderma harzianum* t-22 has been shown to promote plant fitness via secreting small molecules that have diverse functions. Tricholignan A, discovered via genome mining in this work, is a redox-active *ortho*-hydroquinone natural product that can facilitate reductive Fe assimilation in plant. The biosynthesis of the *ortho*-hydroquinone structure by a pair of polyketide synthases (PKSs) requires a critical Cα-methylation step that serves as the programming checkpoint. The responsible standalone methyltransferase requires chaperoning by a fused and inactive acyl carrier protein for activity. The use of an inactive carrier protein to regulate PKS function adds another layer of complexity to this already highly enigmatic family of enzymes.

Author contributions: M.C. and Y.T. designed research; M.C., Q.L., and A.E.Y. performed research; M.C., Q.L., S.-S.G., S.E.J., and Y.T. analyzed data; and M.C. and Y.T. wrote the paper.

The authors declare no conflict of interest.

This article is a PNAS Direct Submission. C.K. is a guest editor invited by the Editorial Board.

[1]To whom correspondence should be addressed. Email: yitang@g.ucla.edu.

This article contains supporting information online at www.pnas.org/lookup/suppl/doi:10.1073/pnas.1819998116/-/DCSupplemental.

Published online March 6, 2019.

carbon backbone (12, 13). The polyketide structure that results is typically precisely crafted to enable a multitude of post-polyketide synthase (PKS) reactions to take place and furnish the final bioactive products. Additional structural complexity can be generated through collaborative efforts between multiple IPKSs, as illustrated in the biosynthesis of sorbicillin and chaetoviridin A (14, 15). In these pathways, a highly reducing IPKS (HRPKS) and a nonreducing IPKS (NRPKS) collaborate in tandem to synthesize a compound with both reduced and aromatic features. Starting from a cryptic tandem IPKS in *T. harzianum* t-22, we report here the discovery of a redox-active *ortho*-hydroquinone molecule tricholignan A **1**. Tricholignan A is able to reduce Fe(III) to Fe(II), and can alleviate iron deficiency phenotypes in the model plant *Arabidopsis thaliana*. We showed the polyketide core structure of tricholignan A is constructed via unique programming rules involving a *trans*-acting MT. Our studies therefore support the potential of genome mining in biofertilizer fungi to afford new agriculturally relevant natural products.

Results

Activating Silent *tln* Cluster in *T. harzianum* t-22 Leads to Tricholignan A. We performed anti-SMASH and bioinformatic analysis of the sequenced *T. harzianum* genome to identify all IPKS-containing biosynthetic gene clusters (16). Of the 25 gene clusters identified, the *tln* gene cluster encoding an HRPKS (TlnA) and an NRPKS (TlnB) attracted our attention (Fig. 1*A*) because: (*i*) there are genes encoding thioesterase (TE), flavin-dependent monooxygenase (FMO), and *O*-MT, which could further expand chemical diversity, and (*ii*) the gene *tlnC* encodes an unusual didomain protein with an N-terminal acyl carrier protein (ACP) and a C-terminal MT. Analysis of its amino acid sequence revealed that while the conserved *S*-adenosylmethionine (SAM) binding and catalytic motifs of the MT domain are present, the phosphopantetheine (pPant) modification site in the ACP domain is DTI, which deviates from the hallmark DSL sequence (17–19) (Fig. 1*B*). Substitution of the serine with threonine raises the possibility that this ACP domain may not be posttranslationally modified with pPant and may be inactive. Hence, the fusion protein encoded was designated as pseudo-ACP-MT (ψACP-MT). RT-PCR analysis showed that the cluster was transcriptionally silent under laboratory conditions (*SI Appendix*, Fig. S2.1), consistent with the strain producing primarily pachybasin, which is unrelated to the *tln* cluster (Fig. 1*C*, *i*). To activate this gene cluster, we use a transcription activation approach (8, 9). The gene *tlnI*, which encodes a putative GAL4-like Zn_2Cys_6 transcription factor, was cloned under the control of the constitutive gpdA promoter (8). Upon integration of this cassette into *T. harzianum* to yield the strain TLB2, transcription of genes in the *tln* cluster was activated (*SI Appendix*, Fig. S2.1).

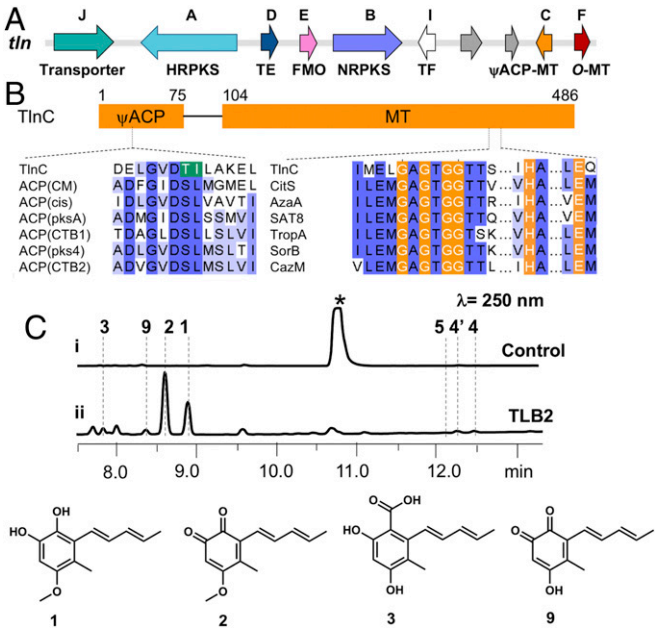

Fig. 1. Genome mining of the redox-active tricholignan from *T. harzianum* t-22. (*A*) Organization of the *tln* gene cluster. TF, transcription factor. (*B*) Domain organization and active site motifs of TlnC. (*C*) Extracted LC traces of metabolite extracts from a control strain (*i*) and TLB2, the *tlnI* overexpression strain (*ii*). The asterisk represents pachybasin.

Several distinctive metabolites emerged from the extract of TLB2 grown in potato dextrose broth for 4 d at 28 °C, with **1** and **2** being the major compounds (~2 mg/L) (Fig. 1*C*). Compounds with similar UV absorbance profiles [λ_{max} (wavelength of maximum absorption) = 222 nm, λ_{max} = 279 nm] were isolated, and the structures were determined by NMR analysis (*SI Appendix*, Tables S4–S8). Tricholignan A **1** is a trisubstituted *o*-hydroquinone (4-methoxy-5-methyl-6-sorbyl *o*-hydroquinone), while tricholignan B **2** is the oxidized *o*-quinone. Compounds **1** and **2** therefore form a redox pair, with **1** undergoing air oxidation to **2**. Both **1** and **2** are compounds not previously reported in the literature.

The minor metabolites identified from TLB2 that are related to **2** are putative precursors (**3** and **9**) and dimers of **1** and **2** (**4**, **4′**, and **5**). Compound **3** is a tetrasubstituted benzoic acid and is proposed to be the product of the HRPKS/NRPKS collaboration (Fig. 1). Compound **3** can undergo oxidative decarboxylation and oxidation to quinone **9** (isolated as a mixture of *o*- and *p*-quinone) (20) (Fig. 1). Compounds **4**, **4′**, and **5** are all heterodimers of **1** and **2**, and are fused by a 1,4-benzodioxin moiety derived from the cycloaddition between the sorbyl chain in **1** and the *o*-quinone in **2** (*SI Appendix*, Fig. S2.2). Such connectivity was observed among plant metabolites, and has been proposed to occur nonenzymatically (21).

Reduction of Fe(III) by Tricholignan A Improves Iron Acquisition by *A. thaliana*. *Ortho*-hydroquinones are known to be redox-active (22). Separate analysis of metabolites in media and cells of *T. harzianum* t-22 showed that **1** and **2** are exported and accumulated extracellularly, suggesting a possible redox role in the environment. Recent studies by Sattely and coworkers (23) showed that hydroxyquinones, such as fraxetin and sideretin secreted by roots of *A. thaliana*, can help the plant assimilate Fe(II) by solubilization and reduction of Fe(III) in soil. The redox potential of the tricholignan pair was measured by cyclic voltammetry. With a standard redox potential (E^0) of 568 mV at pH 6.4 and an E^0 of 545 mV at pH 7.0 (Fig. 2*A* and *SI Appendix*, Fig. S2.3), **1** could serve as a facile electron donor to reduce Fe(III) to Fe(II) (Fig. 2*A*). Indeed, an iron reduction assay coupled with ferrozine showed that **1** was able to reduce Fe(III) (*SI Appendix*, Fig. S2.4). Iron reduction by tricholignan A is slower compared with plant-derived coumarin fraxetin (23), and both reductants are susceptible to air oxidation during iron reduction in vitro.

Having established that **1** can reduce Fe(III) to Fe(II) in vitro, we hypothesized that the observed redox activity might be biologically relevant in facilitating iron acquisition by plants. To test this potential activity of **1**, we selected the *f6′h1-1* mutant (SALK_132418C) of *A. thaliana*, which cannot synthesize scopoletin (the precursor of fraxetin and sideretin), and is therefore defective in reductive iron acquisition (23). *A. thaliana* strictly uses a reduction-based strategy to acquire Fe(II), which separates itself from the other plants that utilize phytosiderophores to chelate Fe(III) (24). Under Fe-deficient conditions, the *f6′h1* mutant exhibits mild chlorosis at pH 5.6 on agar. In the presence of 150 μM tricholignan A, chlorosis was rescued (Fig. 2*B*). Given that chlorophyll content is strongly correlated to the intracellular Fe(II) concentration in plants (25), we determined chlorophyll concentrations of *f6′h1* mutant seedlings under the testing growth conditions. The mean chlorophyll content of *A. thaliana* seedlings when grown in

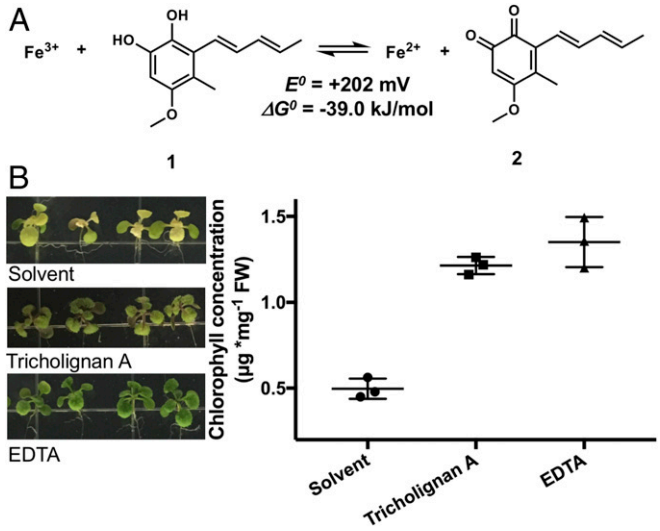

Fig. 2. Tricholignan A can facilitate reductive iron assimilation in *A. thaliana* of model plants. (*A*) Standard free energy changes (ΔG^0) and E^0 for ferric reduction by tricholignan A **1**. The previously reported value of +0.77 V (vs. standard hydrogen electrode) was used for ferric-to-ferrous reduction. (*B*) Phenotypic characterization and complementation assays for *A. thaliana f6′h1* mutant under Fe-deficient conditions.

the presence of tricholignan A was 1.2 μg * mg^{-1} of fresh weight (FW; the unit is defined as chlorophyll concentration in micrograms per milligram of FW leaf disks), which is comparable to that of the positive control of adding EDTA. As expected, the chlorophyll content of the seedlings grown on solvent-only control was significantly lower, at around 0.5 μg * mg^{-1} of FW. A previous study showed that *T. harzianum* t-22 grown in liquid culture can generate diffusible metabolites that reduce Fe(III) to Fe(II) to promote plant growth, but the molecular basis was unknown (26). Our studies suggest genome-mined **1** may be one such metabolite that can reduce Fe(III), while the biosynthesis of **1** may be activated under specific conditions.

Given the potential role of **1** in iron assimilation, we postulated that the *tln* cluster should be found in other beneficial fungal species besides *T. harzianum* t-22. An anti-SMASH search of publicly available sequenced genomes revealed that this cluster is conserved across *Trichoderma* spp., including *Trichoderma virens*, *Trichoderma atrobrunneum*, *Trichoderma guizhouense*, and several other *T. harzianum* variants (2, 27, 28) (*SI Appendix*, Fig. S2.5). These clusters encode proteins that are almost identical to the ones in the *tln* cluster, with amino acid identities of over 80%. These fungi have been reported to promote plant growth, and the fact that the *tln* cluster is conserved in them but absent in other fungal genera further supports its potential role in improving plant fitness.

Reconstitution of Tricholignan A Biosynthesis. The *o*-hydroxyquinone moiety of **1** is essential for the observed redox activity. Searching through known fungal natural products showed that this is rare among fungal metabolites (29). To understand the biosynthetic logic in producing *o*-hydroxyquinone via a polyketide pathway, we reconstituted the individual steps in the biosynthesis of **1** and **2**. We expressed combinations of *tln* genes in *Saccharomyces cerevisiae* BJ5464-NpgA (30) (Fig. 3*B*). Whereas expression of the IPKSs (TlnA and TlnB) alone or together did not yield any detectable products, coexpression of TlnD (TE) led to formation of the truncated pentaketide pyrone **7** as a major product and hexaketide β-resorcylic acid **8** as a minor product. TlnD is therefore proposed to be the TE that releases the products from TlnB via hydrolysis (Fig. 3*A*). Coexpression of TlnC (ψACP-MT) with TlnA, TlnB, and TlnD in yeast resulted in biosynthesis of **3** (Fig. 3*B*), thereby confirming the MT domain is active and is responsible for C5-methylation in **1**–**3**.

Starting from the yeast strain that produced **3**, further coexpression of TlnE (FMO) and TlnF (*O*-MT) produced **2** (~0.2 mg/L). The catalytic roles of TlnE and TlnF were verified using purified enzyme assays (*SI Appendix*, Fig. S2.6). In the presence of both enzymes, NADPH and SAM, **3** is converted to **2** (*SI Appendix*, Fig. S2.6, *v*). The sequence of reactions was established by adding enzymes individually in the assay. Incubating **3** and NADPH with TlnE yielded **9** (and **9′**) (*SI Appendix*, Fig. S2.6, *iii*). We were not able to detect the reduced intermediate **10**, likely due to rapid spontaneous air oxidation. The oxidative decarboxylation of TlnE is similar to that of salicylate hydroxylase in *Pseudomonas putida*, which catalyzes conversion of salicylic acid to catechol (31). Directly incubating **9** and SAM with TlnF led to **2** (*SI Appendix*, Fig. S2.6, *iv*). However, adding TlnF to **3** did not lead to any *O*-methylated products (*SI Appendix*, Fig. S2.6, *ii*), confirming the sequence of reactions as shown in Fig. 3*A*. The enzymatic conversion of **3** to **2** reveals the logic of *o*-quinone biosynthesis: Following oxidative decarboxylation by TlnE, both *o*- and *p*-quinones (**9** and **9′**) can be formed from trihydroxybenzene **10**. Methylation of the C4-phenol in **9** results in exclusive formation of the *o*-quinone **2**, mimicking the strategy used in the chemical syntheses of *o*-quinone (32).

ψACP Is Required for Polyketide Methylation and Biosynthesis of 3. To study in detail the biosynthesis of **3**, we expressed and purified TlnA, TlnB, and TlnD from yeast, as well as TlnC from *Escherichia coli* BL21(DE3) (*SI Appendix*, Fig. S2.15). One-pot enzymatic reaction of these four enzymes, in the presence of malonyl-CoA, NADPH, and SAM, resulted in the formation of

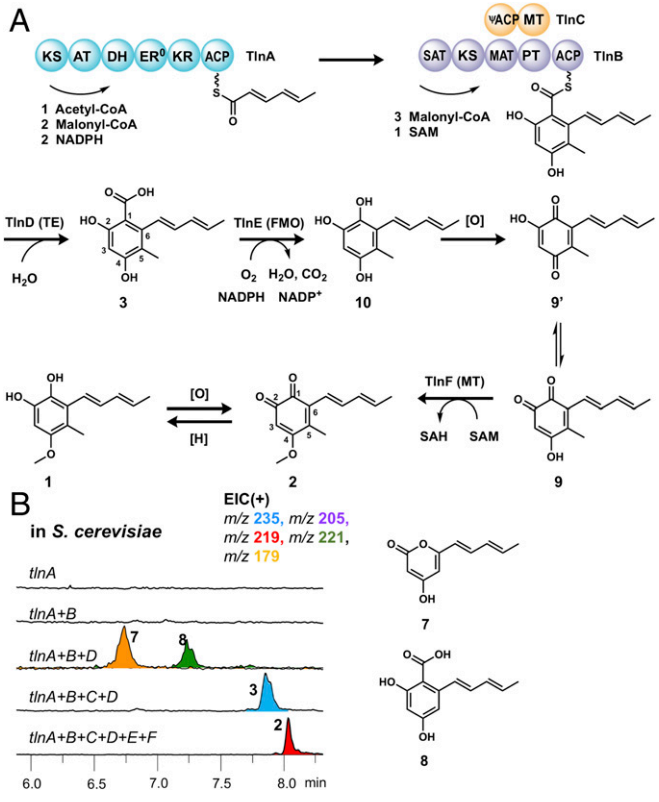

Fig. 3. Functional assignment of enzymes in the *tln* cluster. (*A*) Proposed biosynthetic pathway of the *tln* cluster. AT, acyltransferase; DH, dehydratase; ER, enoylreductase; KR, ketoreductase; PT, product template; SAH, *S*-adenosylhomocysteine. (*B*) Extracted LC/MS traces of reconstitution of TlnA through TlnF activity in *S. cerevisiae* BJ5464-NpgA. EIC, extracted ion chromatogram.

the hexaketide **3** (Fig. 4*B*, *i*), proving these four enzymes are sufficient for biosynthesis of **3**. In the absence of ψACP-MT TlnC, the dominant product synthesized by TlnA, TlnB, and TlnD is **7**, a spontaneously released pentaketide shunt product (Fig. 4*B*, *ii*). Only trace amounts of the 5-desmethyl **8** are formed. When purified TlnC was incubated with **8**, no methylation to **3** can be observed. These results suggest that methylation by the MT domain of TlnC must take place during TlnB-catalyzed chain elongation, and does not take place post-PKS. A proposed scheme of synthesis of **3** by the four enzymes is shown in Fig. 4*A*. The HRPKS TlnA synthesizes the triketide hexa-2,4-dienoate, which can be detected via base hydrolysis of TlnA incubated with malonyl-CoA and NADPH (*SI Appendix*, Fig. S2.7). TlnB accepts the sorbyl unit from TlnA as a starter unit via the starter unit/ACP transacylase (SAT) domain and extends to the tetraketide intermediate, which can be methylated by TlnC. Following two more rounds of chain extension by TlnB to give the hexaketide, the product template domain of TlnB catalyzes regioselective cyclization to yield the TlnB-tethered 2,4-dihydroxybenzoyl product (33, 34). Finally, TlnD catalyzes hydrolytic release to yield **3** (Fig. 4*A*). In the absence of TlnC-catalyzed methylation at the tetraketide stage, TlnB programming rules are derailed and the vast majority of products are released via enolization of the ε-ketone and cyclization to give pyrone **7**. Only a small fraction of unmethylated polyketide can proceed fully to the hexaketide and be released as **8**. Therefore, the TlnC-catalyzed α-methylation step serves as a checkpoint in TlnB programmed steps to ensure **3**, not **8**, is produced. α-Methylation as a checkpoint in HRPKS programming has been noted previously (35, 36), and is observed here for an NRPKS via interacting with an *in trans* MT.

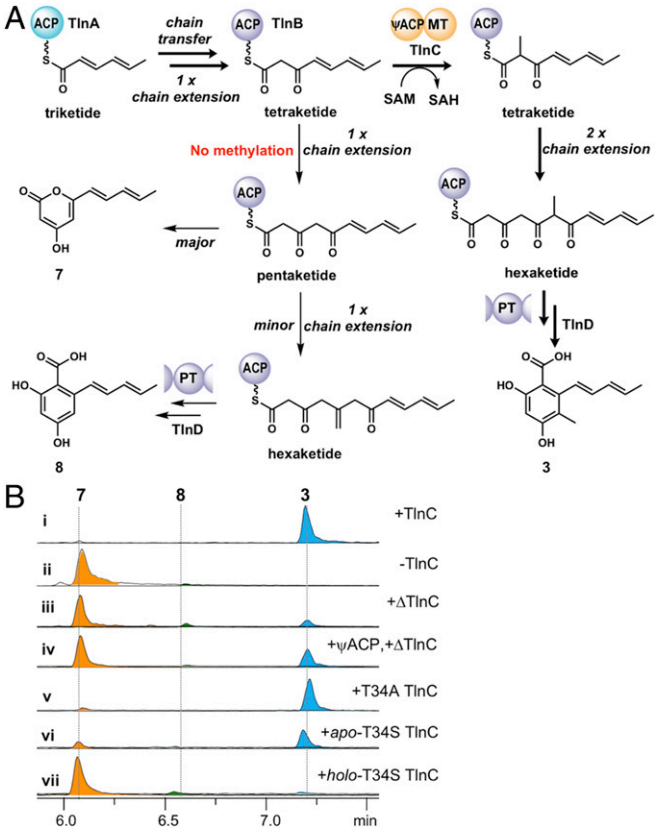

Fig. 4. ψACP in TlnC is essential for formation of **3**. (*A*) Proposed mechanism of TlnC-assisted biosynthesis of **3**. SAH, *S*-adenosylhomocysteine; PT, product template. (*B*) Extracted LC/MS traces of extracts from in vitro reconstitution assays with TlnA, TlnB, TlnD, and different mutants of TlnC. ΔTlnC is the truncated version in which ψACP is removed. The terms *apo* and *holo* indicate the absence and presence of pPant on the ACP domain, respectively. Equimolar enzyme concentrations (20–30 μM) were used in in vitro assays.

To determine the role of the ψACP domain in the TlnC-catalyzed reaction, we excised and assayed the standalone MT domain (ΔTlnC) with TlnA, TlnB, and TlnD. While a small amount of **3** is made, the major product (>80%) is now **7**, indicating the efficiency of methylation is severely impaired without ψACP (Fig. 4*B*, *iii*). This is confirmed through *in trans* complementation with the standalone ψACP domain, which led to a small increase in **3**, but **7** is still a dominant product (Fig. 4*B*, *iv*). Hence, the presence of a fused ψACP significantly enhances the efficiency of the methylation step, possibly via transient protein–protein interactions with TlnB. Increasing the ratio of ψACP to ΔTlnC increased the relative amount of **3** to **7**, although the total polyketide yield decreased (*SI Appendix*, Fig. S2.8).

We then used MALDI-TOF analysis to determine whether the threonine residue present in the DTI motif of ψACP can be posttranslationally modified by the fungal phosphopantetheinyl transferase NpgA (37). When the standalone ψACP was treated with CoA and NpgA, the threonine remained unmodified (*SI Appendix*, Fig. S2.9). In contrast, the excised ACP domain from TlnB (ACP_{cis}) was completely phosphopantetheinylated under the same conditions. The circular dichroism (CD) spectrum of ψACP revealed the characteristic double-negative peaks at 208 nm and 222 nm that are also seen in the CD profile of ACP_{cis} (*SI Appendix*, Fig. S2.10), which are indicative of an intact α-helical bundle structure. Collectively, these data are consistent with a previous study in which introducing a single S36T mutation in *E. coli* FAS ACP led to the abolishment of post-translational modification (17). Therefore, the ψACP domain in TlnC facilitates the *in trans* methylation reaction and may be purposely kept in the *apo* form. This was further demonstrated by using the T34A TlnC mutant in the PKS assay, which produced mostly **3** (>95%) (Fig. 4*B*, *v*).

To evaluate the effects of phosphopantetheinylation of the ψACP domain, we first generated a T34S-ψACP mutant in which the serine residue is reintroduced. The *apo* T34S-ψACP can now be completely converted into the *holo* form by NpgA in vitro (*SI Appendix*, Fig. S2.9), thereby supporting that the threonine residue in ψACP is present to keep the ACP domain in the *apo* form. We then introduced the T34S mutation into the full-length TlnC and repeated the PKS assays. The *apo* form of T34S TlnC was slightly compromised in activity, but still produced **3** as the major product (>70%) (Fig. 4*B*, *vi*). Surprisingly, the MT activities of *holo* T34S-TlnC are nearly completely abolished, as pyrone **7** constituted over 95% of all products, with trace amounts of **8** and **3** (Fig. 4*B*, *vii*). This result confirms that the *apo* form of the ψACP domain is required for proper functioning of the MT domain. Since *holo* T34S-TlnC did not inhibit PKS turnover (as evident in the formation of **7**), we reason that the pPant arm in mutant ψACP may insert into the juxtaposed MT domain active site and effectively inhibit TlnB ACP from shuttling the tetraketide substrate (3-oxo-4,6-octadienoyl) to the MT. The use of an unphosphopantetheinylated ACP ensures that it will not compete with acyl-ACP_{cis} from TlnB for access to TlnC MT. Therefore, the ψACP is a decoy: It is present in the apparent inactive *apo* form and cannot serve as an acyl shuttle of polyketide chains, yet it is critical in facilitating TlnB and TlnC interactions to ensure that the regioselective methylation takes place.

ψACP Inhibits Decarboxylative Condensation by Ketide Synthase Domain to Facilitate Methylation. During nonreducing polyketide chain elongation by NRPKS, premature spontaneous cyclization of the reactive poly–β-ketone chain is suppressed in the active site of the NRPKS. After decarboxylative condensation between the growing polyketide chain attached to the ketide synthase

(KS) domain and an incoming malonyl-ACP, the polyketide chain may be transferred back to the KS domain and remain in the active site tunnel, or leave the active site in the form of acyl-ACP, followed by reentry and transthioesterification (38, 39). In order for MT domains to methylate α-positions, the polyketide chain must be accessible by the MT domains. In most NRPKSs that methylate polyketides, an in-line MT domain immediately fused to the ACP domain allows the MT to be in close proximity to the megasynthase core and to be accessible by acyl-ACP (36, 40). Here, TlnC is a dissociated MT enzyme that must gain access to the tetraketidyl-ACP to perform methylation. We hypothesize that ψACP may bind to TlnB via protein–protein interactions to recruit TlnC to the TlnB reaction core. In addition, ψACP may bind to the entrance of the KS active site and slow down the reentry of the tetraketidyl-ACP_{cis} before methylation (Fig. 5*D*). In this case, an increased ratio of ψACP to TlnB should inhibit NRPKS activity, which was observed in the *in trans* complementation assay of ΔTlnC (*SI Appendix*, Fig. S2.8).

To test these hypotheses, we dissected TlnB into its minimal PKS component of ACP_{cis} and SAT-KS-MAT^0, in which the malonyl acyl transferase (MAT) domain is deactivated. Working with minimum PKS allowed us to achieve higher expression of the dissected proteins for assays (36), and provides a direct examination of the effects of ψACP on the extension step from tetraketide to pentaketide, after which pyrone **7** is the expected product. We performed a single-round chain extension assay in which the tetraketide **10** was used as a starter unit to prime the KS domain (Fig. 5*A*). Malonyl-ACP_{cis} was generated by preloading malonyl-CoA on *apo*-ACP_{cis} with NpgA. Using preloaded malonyl-ACP_{cis} together with SAT-KS-MAT^0 can exclude any possible ψACP–MAT interactions in the assay. In the presence of an increasing amount of ψACP relative to SAT-KS-MAT^0 and malonyl-ACP_{cis}, the yield of **7** significantly decreases (Fig. 5*B*), confirming that ψACP can inhibit a chain extension event catalyzed by KS. We next compared the inhibitory activities of ψACP-MT on minimal PKS with *apo*-ACP_{cis} and a noncognate *apo*-ACP from the NRPKS CazM (15). Likewise, we isolated the chain extension event from tetraketide to pentaketide by using minimal PKS SAT-KS-MAT and ACP_{cis}, and used tetraketide **10** to prime the KS domain. Here, the MAT was kept active so that multiple turnovers could take place to accumulate pyrone **7**. In contrast to the strong inhibition observed with ψACP-MT, titrating *apo*-ACP_{cis} or noncognate ACP to TlnB minimal PKS led to only a moderate decrease in the yield of **7** (Fig. 5*C* and *SI Appendix*, Fig. S2.11).

Based on the recent structure of CTB1, which is an NRPKS synthesizing *nor*-toralactone (39), we propose a model of TlnC ψACP-MT interacting with TlnB NRPKS (Fig. 5*D*). Similar to known ACPs, multiple negatively charged residues are distributed throughout the first half of the ψACP sequence. These charges were shown to mediate protein–protein interactions between ACP and the PKS core (38) (*SI Appendix*, Fig. S2.12). In our model, ψACP binds to the KS domain via similar electrostatic interactions and promotes departure of tetraketidyl-ACP_{cis} from the KS active site and methylation by TlnC; following methylation, methylated tetraketidyl-ACP_{cis} enters the KS domain for the next extension step. Previous findings showed that each catalytic step in IPKS machineries is a result of kinetic competition between functional domains (35, 40). Here, the dissociated nature of the TlnC MT has a lower effective concentration compared with its in-line counterparts (41). To compensate for the kinetic loss, a decoy ψACP is recruited to slow down KS-catalyzed chain elongation, while providing protein–protein interactions to facilitate TlnC MT functions.

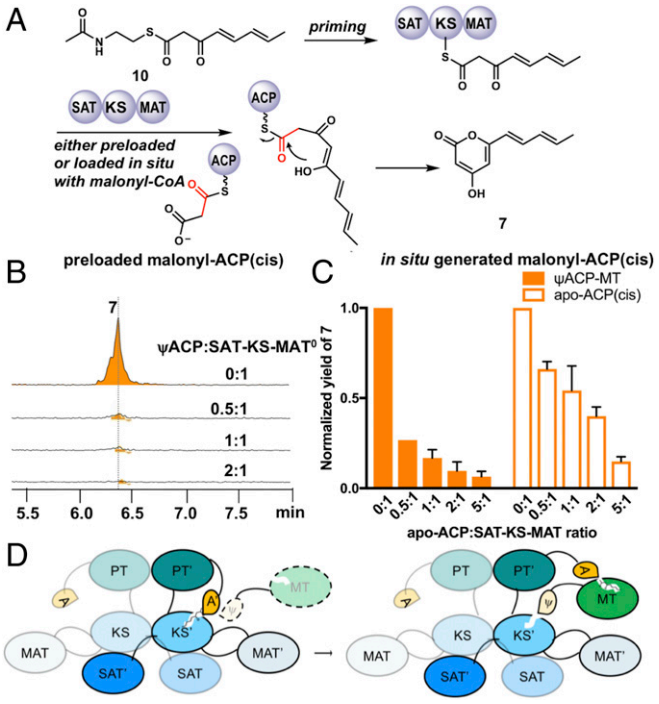

Fig. 5. ψACP inhibits KS to allow for methylation by TlnC *in trans*. (*A*) Minimum TlnB PKS primed with **10** leads to the formation of **7**. (*B*) When using malonyl-ACP_{cis}, increasing the molar ratio of ψACP to SAT-KS-MAT^0 decreases formation of **7**. (*C*) Inhibition of minimal TlnB PKS by ψACP-MT is significant. (*D*) Proposed model of the role of ψACP in facilitating methylation of 3-oxo-4,6-octadienoyl ACP_{cis} by TlnC. PT, product template.

Discussion

T. harzianum t-22, widely used as a biofertilizer and biocontrol fungus, utilizes small molecules to enable chemical communication with neighboring plants (11). Many of the *T. harzianum* t-22 biosynthetic clusters are silent under laboratory conditions, and are not associated with known natural products. We activated the transcription of a silent IPKS cluster of interest that led to the production of a pair of unique redox active molecules **1** and **2**. Selection of the target cluster was driven by an intriguing collection of biosynthetic enzymes, including the tandem IPKSs and the ψACP-MT fusion protein. Production of the sorbyl-hydroquinone **1** was not anticipated a priori, and underscores the potential of using genome mining to find new natural products. Importantly, we showed **1** can readily reduce Fe(III) to Fe(II) under physiological conditions, and can help *A. thaliana* reductively assimilate Fe(III). Small diffusible molecules produced by *T. harzianum* t-22 were previously shown to reduce Fe(III) to Fe(II) (26), and **1** may therefore be one such molecule. Although the exact role of **1** in fungal host physiology is unknown, our work shows that identifying these compounds and elucidating their mechanisms can accelerate the development of new natural products in agriculture.

Our work here also unveiled unique programming features of fungal NRPKS. TlnC is an example in thiol template biosynthesis (PKS and NRPS) that an inactive ACP plays an important role. The nonphosphopantetheinylated nature of ψACP renders it incapable of shuttling polyketide intermediates and eliminates competition with ACP_{cis} for the TlnC active site. However, the intact ACP tertiary structure and conserved surface charge residues allow the *apo*-ACP to inhibit decarboxylative condensation, possibly through interacting with the KS domain. Such binding may hinder the reentry of the tetraketide-ACP to the KS domain and allow it to be methylated by the MT domain.

The fused ψACP domain provides kinetic benefits to the methylation step. Methylation by ΔTlnC without the fused ψACP is less efficient, as shown by the product ratio of pyrone **7** and **3** (Fig. 4*B*, *iii*), which implies that the MT alone is not kinetically competent enough to compensate for its dissociation from NRPKS. In fact, it appears that TlnC methylation activity may be

intrinsically slower compared with other in-line MTs. A recent study on citrinin PksCT shows that equimolar complementation of its in-line MT *in trans* almost completely restores the polyketide methylation pattern (40). The fusion of ψACP can establish protein–protein interactions between TlnC and NRPKS TlnB. As a result, the MT can be recruited to the NRPKS and minimize the exposure of the reactive poly–β-ketone chain to solvent.

The NRPKS machinery in the *tln* cluster essentially has two ACPs, with one catalytically inactive but functionally essential. This is in contrast to NRPKSs, which use two catalytically active and functionally equivalent ACPs, as in the case of CTB1 and naphthopyrone synthase wA (39, 42). Such tandemly arranged *holo*-ACPs are synergetic in shuttling acyl intermediates into different functional domains to improve biosynthetic efficiency (43). Therefore, tandem *holo*-ACPs and ψACP may represent different time points during NRPKS evolution: Gene duplication yielded tandem ACPs in NRPKS, while later gene fission and mutation afforded ψACP the opportunity to play more of a structural and regulatory role (44, 45) (*SI Appendix*, Fig. S2.13). A genome survey of other sequenced fungi reveals that additional ψACP fusion to polyketide-modifying enzymes can be found in cryptic PKS gene clusters (*SI Appendix*, Fig. S2.14). These ψACP fusion enzymes may employ hitherto unknown programming rules in the biosynthesis of new natural products.

Conclusions

We discovered redox-active *o*-hydroquinone tricholignan A **1** from biofertilizer fungus *T. harzianum* t-22 via a genome mining approach. Tricholignan A can reduce Fe(III) to Fe(II), and may be among the molecules that are synthesized by *T. harzianum* t-22 in soil and help plants acquire Fe(II). Tricholignan A is synthesized by a tandem PKS pair, with the additional assistance of an unusual ψACP-MT fusion protein. The ψACP, which must be kept in *apo* form, is proposed to interact with the PKS to enhance access of the MT domain to the polyketide substrate. This study reveals unique natural products from fungi that benefit plant fitness, as well as unusual biosynthetic logic by IPKSs.

Materials and Methods

Analyses of fungal and yeast metabolic profiles and enzymatic reactions were monitored by liquid chromatography (LC)/MS with a Phenomenex Kinetex LC column. All enzymatic reactions were conducted at room temperature. Additional procedures are detailed in *SI Appendix*.

ACKNOWLEDGMENTS. We thank Dr. J. Clardy for providing *T. harzianum* t-22 strain and Dr. E. Sattely for providing *A. thaliana f6′h1* mutant seeds. We thank Dr. F. Liu for assistance with cyclic voltammetry and Drs. R. Giehl and Y. Hai for constructive discussion. This work was supported by NIH Grant 1R35GM118056 (to Y.T.) Chemical characterization studies were supported by shared instrumentation grants from the National Science Foundation (Grant CHE-1048804).

1. Lorito M, Woo SL, Harman GE, Monte E (2010) Translational research on *Trichoderma*: From 'omics to the field. *Annu Rev Phytopathol* 48:395–417.
2. Contreras-Cornejo HA, Macías-Rodríguez L, Cortés-Penagos C, López-Bucio J (2009) *Trichoderma virens*, a plant beneficial fungus, enhances biomass production and promotes lateral root growth through an auxin-dependent mechanism in Arabidopsis. *Plant Physiol* 149:1579–1592.
3. Sivan A, Ucko O, Chet I (1987) Biological control of Fusarium crown rot of tomato by *Trichoderma harzianum* under field conditions. *Plant Dis* 71:587–592.
4. Pusztahelyi T, Holb IJ, Pócsi I (2015) Secondary metabolites in fungus-plant interactions. *Front Plant Sci* 6:573.
5. Stringlis IA, Zhang H, Pieterse CMJ, Bolton MD, de Jonge R (2018) Microbial small molecules–Weapons of plant subversion. *Nat Prod Rep* 35:410–433.
6. Hart MM, et al. (2017) Fungal inoculants in the field: Is the reward greater than the risk? *Funct Ecol* 32:126–135.
7. Brakhage AA (2013) Regulation of fungal secondary metabolism. *Nat Rev Microbiol* 11:21–32.
8. Bergmann S, et al. (2007) Genomics-driven discovery of PKS-NRPS hybrid metabolites from *Aspergillus nidulans*. *Nat Chem Biol* 3:213–217.
9. Sato M, et al. (2017) Collaborative biosynthesis of maleimide- and succinimide-containing natural products by fungal polyketide megasynthases. *J Am Chem Soc* 139:5317–5320.
10. Harman GE (2000) Myths and dogmas of biocontrol changes in perceptions derived from research on *Trichoderma harzinum* t-22. *Plant Dis* 84:377–393.
11. Contreras-Cornejo HA, Macías-Rodríguez L, del-Val E, Larsen J (2016) Ecological functions of *Trichoderma* spp. and their secondary metabolites in the rhizosphere: Interactions with plants. *FEMS Microbiol Ecol* 92:fiw036.
12. Chooi YH, Tang Y (2012) Navigating the fungal polyketide chemical space: From genes to molecules. *J Org Chem* 77:9933–9953.
13. Simpson TJ (2014) Fungal polyketide biosynthesis–A personal perspective. *Nat Prod Rep* 31:1247–1252.
14. al Fahad A, et al. (2014) Oxidative dearomatisation: The key step of sorbicillinoid biosynthesis. *Chem Sci* 5:523–527.
15. Winter JM, et al. (2012) Identification and characterization of the chaetoviridin and chaetomugilin gene cluster in *Chaetomium globosum* reveal dual functions of an iterative highly-reducing polyketide synthase. *J Am Chem Soc* 134:17900–17903.
16. Weber T, et al. (2015) antiSMASH 3.0-a comprehensive resource for the genome mining of biosynthetic gene clusters. *Nucleic Acids Res* 43:W237-43.
17. Keating DH, Carey MR, Cronan JE, Jr (1995) The unmodified (apo) form of *Escherichia coli* acyl carrier protein is a potent inhibitor of cell growth. *J Biol Chem* 270:22229–22235.
18. Flugel RS, Hwangbo Y, Lambalot RH, Cronan JE, Jr, Walsh CT (2000) Holo-(acyl carrier protein) synthase and phosphopantetheinyl transfer in *Escherichia coli*. *J Biol Chem* 275:959–968.
19. Crawford JM, Vagstad AL, Ehrlich KC, Udwary DW, Townsend CA (2008) Acyl-carrier protein-phosphopantetheinyltransferase partnerships in fungal fatty acid synthases. *ChemBioChem* 9:1559–1563.
20. Hlouchova K, Rudolph J, Pietari JM, Behlen LS, Copley SD (2012) Pentachlorophenol hydroxylase, a poorly functioning enzyme required for degradation of pentachlorophenol by *Sphingobium chlorophenolicum*. *Biochemistry* 51:3848–3860.
21. Biedermann D, Vavříková E, Cvak L, Křen V (2014) Chemistry of silybin. *Nat Prod Rep* 31:1138–1157.
22. Steenken S, Neta P (1982) One-electron redox potentials of phenols. Hydroxy- and aminophenols and related compounds of biological interest. *J Phys Chem* 86:3661–3667.
23. Rajniak J, et al. (2018) Biosynthesis of redox-active metabolites in response to iron deficiency in plants. *Nat Chem Biol* 14:442–450.
24. Kobayashi T, Nishizawa NK (2012) Iron uptake, translocation, and regulation in higher plants. *Annu Rev Plant Biol* 63:131–152.
25. Spiller S, Terry N (1980) Limiting factors in photosynthesis: II. Iron stress diminishes photochemical capacity by reducing the number of photosynthetic units. *Plant Physiol* 65:121–125.
26. Altomare C, Norvell WA, Bjorkman T, Harman GE (1999) Solubilization of phosphates and micronutrients by the plant-growth-promoting and biocontrol fungus *trichoderma harzianum* rifai 1295-22. *Appl Environ Microbiol* 65:2926–2933.
27. Zhang J, et al. (2016) The neutral metallopeptidase NMP1 of Trichoderma guizhouense is required for mycotrophy and self-defence. *Environ Microbiol* 18:580–597.
28. Chirino-Valle I, et al. (2016) Potential of the beneficial fungus Trichoderma to enhance ecosystem-service provision in the biofuel grass *Miscanthus x giganteus* in agriculture. *Sci Rep* 6:25109.
29. Hashimoto M, Nonaka T, Fujii I (2014) Fungal type III polyketide synthases. *Nat Prod Rep* 31:1306–1317.
30. Ma SM, et al. (2009) Complete reconstitution of a highly reducing iterative polyketide synthase. *Science* 326:589–592.
31. Suzuki K, Katagiri M (1981) Mechanism of salicylate hydroxylase-catalyzed decarboxylation. *Biochim Biophys Acta* 657:530–534.
32. Huang Z, et al. (2015) A divergent and selective synthesis of *ortho*- and *para*-quinones from phenols. *Tetrahedron* 71:5871–5885.
33. Crawford JM, Townsend CA (2010) New insights into the formation of fungal aromatic polyketides. *Nat Rev Microbiol* 8:879–889.
34. Zhou H, Li Y, Tang Y (2010) Cyclization of aromatic polyketides from bacteria and fungi. *Nat Prod Rep* 27:839–868.
35. Cacho RA, et al. (2015) Understanding programming of fungal iterative polyketide synthases: The biochemical basis for regioselectivity by the methyltransferase domain in the lovastatin megasynthase. *J Am Chem Soc* 137:15688–15691.
36. Storm PA, Herbst DA, Maier T, Townsend CA (2017) Functional and structural analysis of programmed C-methylation in the biosynthesis of the fungal polyketide citrinin. *Cell Chem Biol* 24:316–325.
37. Lee KK, Da Silva NA, Kealey JT (2009) Determination of the extent of phosphopantetheinylation of polyketide synthases expressed in *Escherichia coli* and *Saccharomyces cerevisiae*. *Anal Biochem* 394:75–80.
38. Bruegger J, et al. (2013) Probing the selectivity and protein-protein interactions of a nonreducing fungal polyketide synthase using mechanism-based crosslinkers. *Chem Biol* 20:1135–1146, and erratum (2014) 21:913.
39. Herbst DA, et al. (2018) The structural organization of substrate loading in iterative polyketide synthases. *Nat Chem Biol* 14:474–479.
40. Storm PA, Pal P, Huitt-Roehl CR, Townsend CA (2018) Exploring fungal polyketide C-methylation through combinatorial domain swaps. *ACS Chem Biol* 13:3043–3048.
41. Castellana M, et al. (2014) Enzyme clustering accelerates processing of intermediates through metabolic channeling. *Nat Biotechnol* 32:1011–1018.
42. Fujii I, Watanabe A, Sankawa U, Ebizuka Y (2001) Identification of Claisen cyclase domain in fungal polyketide synthase WA, a naphthopyrone synthase of *Aspergillus nidulans*. *Chem Biol* 8:189–197.
43. Gu L, et al. (2011) Tandem acyl carrier proteins in the curacin biosynthetic pathway promote consecutive multienzyme reactions with a synergistic effect. *Angew Chem Int Ed Engl* 50:2795–2798.
44. Leonard G, Richards TA (2012) Genome-scale comparative analysis of gene fusions, gene fissions, and the fungal tree of life. *Proc Natl Acad Sci USA* 109:21402–21407.
45. Pils B, Schultz J (2004) Inactive enzyme-homologues find new function in regulatory processes. *J Mol Biol* 340:399–404.